FTIR and Mass–Spectrometric Measurements of the Rate Constant for the C6H5 + H2 Reaction

3 **AUTHORS**, INCLUDING:

Igor V Dyakov

Vrije Universiteit Brussel

22 PUBLICATIONS   **350** CITATIONS

FTIR and Mass-Spectrometric Measurements of the Rate Constant for the C_6H_5 + H_2 Reaction

J. Park, I. V. Dyakov, and M. C. Lin*

Department of Chemistry, Emory University, Atlanta, Georgia 30322

Received: July 3, 1997; In Final Form: September 9, 1997[⊗]

The rate constant for the C_6H_5 + H_2 → C_6H_6 + H reaction has been measured by pyrolysis/Fourier transform infrared spectrometry (P/FTIRS) in the temperature range of 548−607 K and by pulsed-laser photolysis/ mass spectrometry (PLP/MS) in the temperature range of 701−1017 K. By P/FTIRS, the reaction was studied by measuring time-resolved concentration profiles of the reactant (C_6H_5NO) and the product (C_6H_6) using highly diluted mixtures of C_6H_5NO in H_2 (with or without Ar dilution). In PLP/MS experiments, the C_6H_5 radical was generated by the photolysis of $C_6H_5COCH_3$ at 193 nm in the presence of several Torr of H_2. The C_6H_5 + H_2 rate constant was determined by the absolute yields of C_6H_6 and $C_6H_5CH_3$ products. The results of these two spectrometric measurements agree closely with our theoretically predicted expression, $k = 5.72 \times 10^4 T^{2.43} \exp(-3159/T)$ cm³/(mol·s) and with that of a shock-tube study by Troe and co-workers (ref 20) in the temperature range of 1050−1450 K. Preliminary kinetic data on the CH_3 + C_6H_5 association reaction are also presented.

I. Introduction

Phenyl radical has been considered as one of the most important reactive species in hydrocarbon combustion chemistry, especially in the formation of polycyclic aromatic hydrocarbons (PAH's) which are pivotal to soot formation in its incipient stages.[1−5] For the kinetic studies of phenyl radical reactions, we have carried out experiments using the cavity ringdown (CRD) technique, covering a typical temperature range of 298−523 K.[6−15] Temperature broadening of the rovibronic transition of C_6H_5 in the visible region limits its kinetic measurements by CRD to about 523 K, above which its S/N ratio deteriorates rapidly with temperature. This temperature limit ($T \leqslant 523$ K) precludes the studying of slower reactions such as C_6H_5 + H_2 and CH_4. In order to circumvent the shortcoming, in this work we employed two complementary methods for the kinetic study of the C_6H_5 + H_2 reaction using pyrolysis/Fourier transform infrared spectrometry (P/FTIRS) and pulsed-laser photolysis/ mass spectrometry (PLP/MS). The methods effectively extend the kinetically useful temperature range to ~1000 K. The latter method has been successfully applied to obtain the rate constant for the recombination reaction of C_6H_5 radicals,[16] and the total rate constants and product branching ratios for the reactions of NH_2 with NO_x.[17,18]

The mechanism of the C_6H_5 + H_2 reaction has been investigated theoretically using a modified Gaussian 2 method (G2M).[19] The reaction was predicted to occur exclusively by direct abstraction with a barrier of 8.8 kcal/mol. The transition state (TS) was found to have a linear C−H−H structure with C_{2v} symmetry. The rate constant calculated according to the predicted geometries and molecular parameters (frequencies and moments of inertia) of the TS and the reactants using transition-state theory (TST) with tunneling corrections was found to be in good accord with the recent shock tube results of Troe and co-workers.[20] Comparison of the theory with the present and other available data in the literature[21−24] will be discussed.
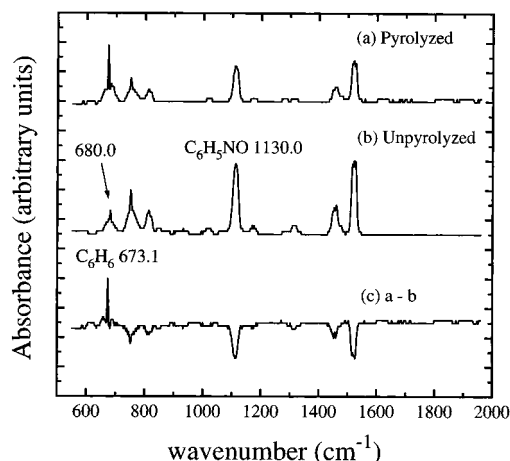

Figure 1. Typical FTIR spectra of pyrolyzed and unpyrolyzed samples.

II. Experimental Section

As alluded to above, two methods complementary to the CRD technique have been developed for the slow abstraction reaction of C_6H_5 with H_2. The experimental procedures of the P/FTIRS and PLP/MS methods have been given previously,[16−18,25,26] and a brief description of each is presented below.

1. P/FTIRS. With this method, C_6H_5NO was used as the phenyl source. Highly diluted mixtures of C_6H_5NO in H_2 (with or without further dilution with Ar) were pyrolyzed in the 548− 607 K temperature range at atmospheric pressure. Pyrolyzed or unpyrolyzed reference samples were expanded into the absorption cell inside the analysis chamber for determination of the concentrations of the C_6H_6 product and the unreacted C_6H_5NO reactant. The pressures of the samples after expansion are approximately 270 Torr. To minimize the effect of pressure-broadening, the pressure of calibration mixtures containing varying amounts of C_6H_6 and C_6H_5NO was maintained at 270 ± 10 Torr. Absorption peaks at 673.1 and 1130.0 cm⁻¹ were employed for the determination of C_6H_6 and C_6H_5NO, respectively.

Figure 1 presents typical FTIR spectra for pyrolyzed and unpyrolyzed samples. This set of spectra illustrates that the
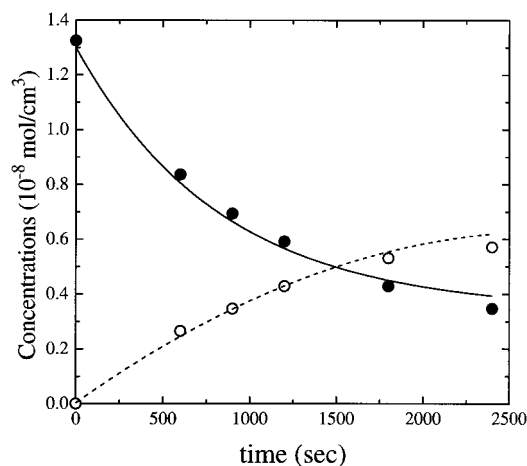
---

* Corresponding author. E-mail: chemmcl@emory.edu.

Figure 2. Time-resolved C_6H_5NO decay (solid points) and C_6H_6 formation (open circles) profiles in P/FTIR experiments at $T = 598$ K. Lines are the modeled results. Reaction conditions are given in Table 1.

TABLE 1: Experimental Conditions[a] and Modeled Rate Constants in P/FTIR Experiment for the Reaction of C_6H_5 + H_2 at Temperatures Studied

| T (K)	$[C_6H_5NO]_0$	$[Ar]_0$	$[H_2]_0$	k_4 (cm³/mol·sec)[b]
548	1.70×10^{-8}	0.00×10^{-5}	2.22×10^{-5}	7.45×10^8
558	1.43×10^{-8}	1.17×10^{-5}	1.02×10^{-5}	$(1.18 \pm 0.66) \times 10^9$
563	1.58×10^{-8}	1.04×10^{-5}	1.13×10^{-5}	1.14×10^9
573	1.55×10^{-8}	1.02×10^{-5}	1.11×10^{-5}	$(1.20 \pm 0.18) \times 10^9$
583	1.53×10^{-8}	1.00×10^{-5}	1.09×10^{-5}	$(1.44 \pm 0.15) \times 10^9$
589	1.35×10^{-8}	1.10×10^{-5}	9.64×10^{-6}	$(1.35 \pm 0.14) \times 10^9$
598	1.33×10^{-8}	1.09×10^{-5}	9.49×10^{-6}	$(1.48 \pm 0.20) \times 10^9$
607	1.31×10^{-8}	1.07×10^{-5}	9.35×10^{-6}	$(1.99 \pm 0.13) \times 10^9$

[a] The concentration units are in mol/cm³. [b] For each temperature (except 548 and 563 K), typically 3–5 runs were carried out. The uncertainty represents 1σ.

major absorption peaks of the reactant and product are clearly separated. The C_6H_6 peak at 673.1 cm overlaps with a small peak of C_6H_5NO; the overlap can be readily corrected. Figure 2 shows a typical set of the concentration vs time plots for the formation of C_6H_6 and the decay of C_6H_6NO. The corresponding curves represent kinetically modeled values. The values of the rate constant for C_6H_5 + H_2 obtained by modeling are summarized in Table 1. The mechanism employed for modeling will be discussed later.

2. PLP/MS. By the mass-spectrometric method, the pulsed photolysis of $C_6H_5COCH_3$ at 193 nm was employed as the C_6H_5 radical source. $C_6H_5COCH_3$, carried by an excess amount of He was premixed in corrugated stainless steel tubing with H_2 before being introduced in the Saalfeld-type quartz reactor[27,28] which can be heated to 1200 K. The reactants and the products of the photoinitiated reaction were supersonically sampled and ionized by electron-impact ionization. The mole fraction of $C_6H_5COCH_3$ was typically <0.5% and that of H_2 >75%, with $[H_2]/[C_6H_5COCH_3] > 150$. The conversion of $C_6H_5COCH_3$ by the unfocused ArF laser beam ranged from 15% to 40%. The mechanism for the fragmentation of $C_6H_5COCH_3$ at 193 nm has been studied by using NO or HBr as the C_6H_5 radical scavengers.[29] The kinetic modeling of measured yields of C_6H_5-NO or C_6H_6 and CH_4 under fully inhibited conditions revealed that ~80% of the fragmentation reaction gave rise to C_6H_5. This result is consistent with the measured yield of $C_6H_5CH_3$ without NO or HBr. The introduction of an excess amount of NO, for example, eliminated the formation of toluene.[29]

In the absence of H_2, the major molecular products from the $C_6H_5COCH_3$ photolysis were $C_6H_5CH_3$, C_2H_6 and $C_{12}H_{10}$ (which was not quantitatively determined in this study), with a

trace amount of C_6H_6. Addition of H_2 to the system noticeably reduced the yields of $C_{12}H_{10}$ and $C_6H_5CH_3$, with a concomitant increase in the yield of C_6H_6. Table 2 summarizes the experimental conditions employed and the yields of C_6H_6 and $C_6H_5CH_3$ measured in the PLP/MS experiment. Kinetic modeling of the absolute concentrations of these products, determined by careful calibrations using standard mixtures sampled at the same total pressure employed in each run, gave the rate constants for the formation of C_6H_6 and $C_6H_5CH_3$ by the following respective reaction:

$$C_6H_5 + H_2 \rightarrow C_6H_6 + H$$

$$C_6H_5 + CH_3 \rightarrow C_6H_5CH_3$$
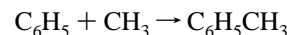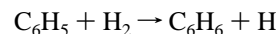
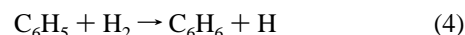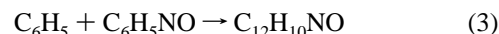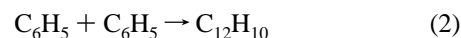CH_4 is present in these experiments in a much lower concentration than C_6H_6 and was presumed to be formed by the CH_3 + $H_2 \rightarrow CH_4$ + H reaction. The comparison of the measured and predicted yields will be discussed in the following section.

III. Results and Discussion

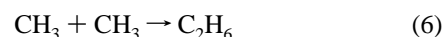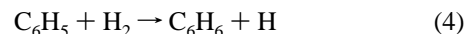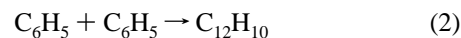**1. Kinetics of the C_6H_5 + H_2 Reaction.** The rate constant of the C_6H_5 + H_2 reaction can be obtained by kinetic modeling in a straightforward manner. The mechanisms employed for the modeling are presented in Tables 3 and 4 for the pyrolysis of $C_6H_5NO-H_2$ mixtures and the photolysis of $C_6H_5COCH_3-$ H_2 mixtures, respectively.

In the thermally initiated C_6H_5NO and H_2 reaction, the formation of C_6H_6 was influenced by the following primary processes:

$$C_6H_5NO = C_6H_5 + NO \qquad (1, -1)$$

$$C_6H_5 + C_6H_5 \rightarrow C_{12}H_{10} \qquad (2)$$

$$C_6H_5 + C_6H_5NO \rightarrow C_{12}H_{10}NO \qquad (3)$$

$$C_6H_5 + H_2 \rightarrow C_6H_6 + H \qquad (4)$$

All but reaction 4 have been determined recently by us.[16,26] The results of our sensitivity analysis (see Figure 3) bear this out. In order to account for the loss of C_6H_5, several secondary and tertiary reactions were included in the modeling, employing "reasonably" assumed values of radical–radical reaction rate constants (see Table 3). The values of rate constant for the C_6H_5 + H_2 reaction are presented in Table 1 and Figure 5 (vide infra).

In the photoinitiated reaction of $C_6H_5COCH_3$ in the presence of excess amounts of H_2, the production of C_6H_6 was found to be influenced by the following primary processes:

$$C_6H_5 + C_6H_5 \rightarrow C_{12}H_{10} \qquad (2)$$

$$C_6H_5 + H_2 \rightarrow C_6H_6 + H \qquad (4)$$

$$C_6H_5 + CH_3 \rightarrow C_6H_5CH_3 \qquad (5)$$

$$CH_3 + CH_3 \rightarrow C_2H_6 \qquad (6)$$

The result of sensitivity analysis carried out at 887 K (see Figure 4) clearly bears this out. Again, in order to minimize the loss of C_6H_5 in our simulation, several secondary and tertiary reactions were included in the model as shown in Table 4. A sensitivity analysis of this system shown in Figure 4 reveals that the yield of C_6H_6 is most strongly and positively affected by reaction 4 and negatively influenced by its competitive reactions 2 and 5.

Rate Constant for the C$_6$H$_5$ + H$_2$ Reaction

J. Phys. Chem. A, Vol. 101, No. 47, 1997 **8841**

TABLE 2: Experimental Conditions^a and Product Yields^b in the PLP/MS Experiment at the Temperatures Studied

temp (K)	P (Torr)	[C$_6$H$_5$COCH$_3$]$_0$	[C$_6$H$_5$]$_0$	[He]$_0$	[H$_2$]$_0$	[C$_6$H$_6$]$_t$ expt	model	[C$_6$H$_5$CH$_3$]$_t$ expt	model
701	3.57	3.66	1.38	126	682	0.35	0.35	0.38	0.38
751	3.66	3.59	1.23	121	654	0.41	0.41	0.29	0.31
811	3.74	1.19	0.97	115	623	0.42	0.42	0.23	0.23
833	3.70	3.41	0.98	110	596	0.47	0.47	0.20	0.19
887	3.00	1.30	0.30	122	419	0.20	0.20	0.04	0.05
888	3.78	1.37	0.90	104	575	0.46	0.46	0.20	0.20
904	3.00	1.27	0.30	119	411	0.21	0.21	0.04	0.04
975	3.00	1.18	0.28	111	381	0.23	0.22	0.03	0.03
1007	3.62	1.24	0.59	88	486	0.40	0.40	0.10	0.09
1017	3.00	1.56	0.24	106	365	0.20	0.19	0.02	0.02

^{a} All concentrations are in units of 10^{-10} mol/cm^3. ^{b} Product yields were measured at $t = 15$ ms in their plateau regions. Typically 3−5 runs were carried out for each temperature. To avoid congestion, the kinetically modeled values of k_4 from the C$_6$H$_6$ yields are summarized in Figure 4 and those of k_5 from the C$_7$H$_8$ yields are given in the text.

TABLE 3: Reactions and Rate Constants^a Used in the Modeling of the C$_6$H$_5$ + H$_2$ Reaction in the P/FTIR Experiment

reactions	A	n	E$_a$	ref
key reactions				
1. C$_6$H$_5$NO = C$_6$H$_5$ + NO	1.42E+17^b	0.00	55060	26
2. C$_6$H$_5$ + C$_6$H$_5$ = C$_{12}$H$_{10}$	1.39E+13	0.00	111	16
3. C$_6$H$_5$ + C$_6$H$_5$NO → C$_{12}$H$_{10}$NO	4.90E+12	0.00	68	16
4. C$_6$H$_5$ + H$_2$ → C$_6$H$_6$ + H	5.72E+04	2.43	6276	19
minor reactions				
7. C$_{12}$H$_{10}$NO → C$_6$H$_5$NO + C$_6$H$_5$	5.00E+14	0.00	45000	c
8. C$_{12}$H$_{10}$NO + C$_6$H$_5$ → C$_{12}$H$_{10}$N + C$_6$H$_5$O	1.00E+12	0.00	0	c
9. C$_6$H$_5$NO + H → C$_6$H$_6$ + NO	4.00E+13	0.00	4310	c
10. C$_6$H$_5$NO + H → C$_6$H$_5$ + HNO	1.00E+12	0.00	0	c
11. C$_6$H$_5$ + C$_6$H$_5$NO → C$_{12}$H$_{10}$ + NO	5.00E+12	0.00	4500	c
12. C$_6$H$_5$ + H → C$_6$H$_6$	7.80E+13	0.00	0	31
13. C$_{12}$H$_{10}$N + NO → C$_{12}$H$_{10}$NNO	1.00E+13	0.00	0	c
14. H + NO + M = HNO + M	5.40E+15	0.00	596	31

^{a} Rate constants are defined by $k = AT^n \exp(-E_a/RT)$ and in units cm^3, mol, and s; E_a is in the units of cal/mol. ^{b} Read as 1.42×10^{17}. ^{c} Assumed.

TABLE 4: Reactions and Rate Constants^a Used in the Modeling of the C$_6$H$_5$ + H$_2$ Reaction in the PLP/MS Experiment

reactions	A	n	E$_a$	ref
key reactions				
2. C$_6$H$_5$ + C$_6$H$_5$ = C$_{12}$H$_{10}$	1.39E+13^b	0.00	111	16
4. C$_6$H$_5$ + H$_2$ = C$_6$H$_6$ + H	5.72E+04	2.43	6276	19
5. C$_6$H$_5$ + CH$_3$ = C$_6$H$_5$CH$_3$	1.38E+14	−0.30	0	30
6. CH$_3$ + CH$_3$ = C$_2$H$_6$	1.50E+15	−0.64	0	30
minor reactions				
15. C$_6$H$_5$ + H = C$_6$H$_6$	7.80E+13	0.00	0	30
16. CH$_3$ + H$_2$ = CH$_4$ + H	2.89E+02	3.12	8710	32
17. C$_6$H$_5$ + C$_6$H$_5$COCH$_3$ → C$_6$H$_6$ + C$_6$H$_5$COCH$_2$	3.39E+11	0.00	5890	33
18. C$_6$H$_5$ + CH$_4$ → C$_6$H$_6$ + CH$_3$	7.94E+11	0.00	11100	33
19. CH$_3$ + C$_6$H$_5$COCH$_3$ → CH$_4$ + C$_6$H$_5$COCH$_2$	5.01E+10	0.00	7400	33
20. C$_6$H$_5$ + C$_6$H$_5$COCH$_3$ → C$_{12}$H$_{10}$ + CH$_3$CO	3.39E+09	0.00	5890	33
21. C$_6$H$_5$ + C$_6$H$_5$COCH$_3$ → C$_{12}$H$_{10}$COCH$_3$	1.00E+11	0.00	4000	c
22. C$_6$H$_5$COCH$_2$ + CH$_3$ = C$_6$H$_5$COC$_2$H$_5$	5.00E+12	0.00	0	c
23. C$_6$H$_5$COCH$_2$ + C$_6$H$_5$ → C$_{12}$H$_{10}$COCH$_2$	5.00E+12	0.00	0	c
24. C$_6$H$_5$COCH$_2$ + C$_6$H$_5$COCH$_2$ → (C$_6$H$_5$COCH$_2$)$_2$	1.00E+12	0.00	0	c
25. C$_6$H$_5$COCH$_2$ → C$_6$H$_5$ + CH$_2$CO	4.00E+14	0.00	29400	c
26. C$_{12}$H$_{10}$COCH$_3$ → C$_{12}$H$_{10}$ + CH$_3$CO	1.00E+08	0.00	0	c
27. CH$_3$ + CH$_3$CO = CH$_3$COCH$_3$	4.04E+15	−0.80	0	32
28. CH$_3$CO + M = CH$_3$ + CO + M	8.74E+42	−8.62	22420	32

^{a} Rate constants are defined by $k = AT^n \exp(-E_a/RT)$ and in units cm^3, mol, and s; E_a is in the units of cal/mol. ^{b} Read as 1.39×10^{13}. ^{c} Assumed.

The kinetically modeled values of k_4 based on the absolute yields of C$_6$H$_6$ are summarized in Figure 5 for comparison with those obtained by FTIR spectrometry and by Troe and co-workers using UV absorption spectrometry carried out in a shock tube at temperatures between 1050 and 1450 K.[20] The three independent, more direct measurements agree closely with our theoretically predicted values covering the entire temperature range investigated, 548−1450 K.[19] In the figure, we also compare these three sets of experimental data and the theoretically predicted curve with the existing, mostly kinetically

modeled results obtained by shock-heating of C$_6$H$_6$ at high temperatures.[21−23] Among them, the data of laser schlieren measurements by Kiefer and co-workers[23] agree most closely with the theory.

Also included in the figure are the data obtained by Fielding and Pritchard[21] with a relative rate method using the C$_6$H$_5$ recombination reaactin as the reference standard. The relative rate data, after being converted to absolute values with our C$_6$H$_5$ recombination rate constant[17] appear to be much lower than our FTIR and theoretically predicted results.
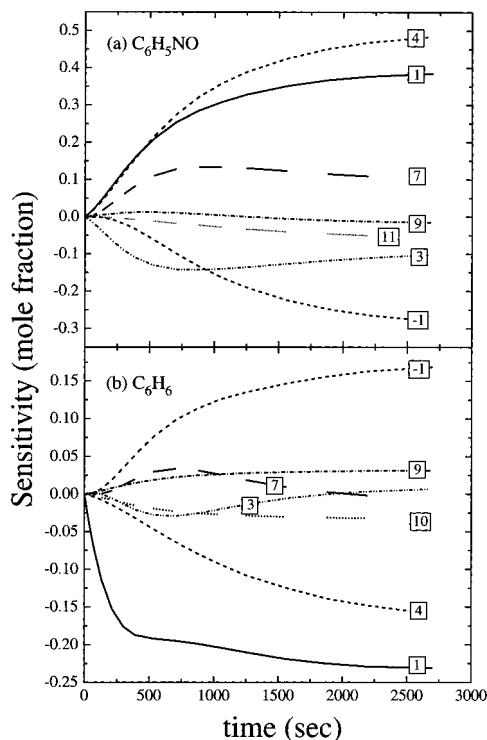
Figure 3. Sensitivity analysis at $T = 589$ K for C_6H_6 and C_6H_5NO in a P/FTIRS experiment.
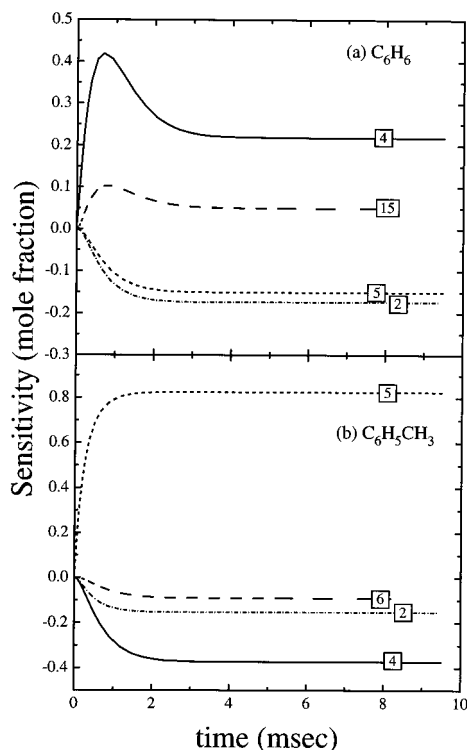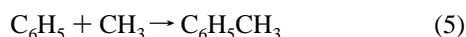

Figure 4. Sensitivity analysis at $T = 887$ K for C_6H_6 and $C_6H_5CH_3$ in a PLP/MS experiment.

2. Kinetics of the $CH_3 + C_6H_5$ Association Reaction. The absolute yield of toluene measured in the present experiment can be directly utilized for estimation of the rate constant for the association reaction:

$$C_6H_5 + CH_3 \rightarrow C_6H_5CH_3 \qquad (5)$$

The values of k_5 obtained by kinetic modeling lie in the range of $(1.8 \pm 0.2) \times 10^{13}$ cm^3/(mol·s) at $701-1017$ K. These values
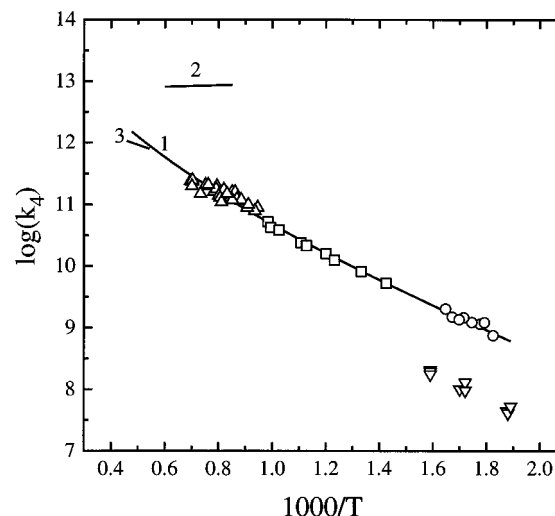

Figure 5. Arrhenius plot of the rate constant for the $C_6H_5 + H_2$ reaction. $\bigcirc$, this work by P/FTIRS; $\square$, this work by PLP/MS; $\triangle$, ref 20; 1, theoretical results of Mebel et al., ref 19; 2, ref 22; 3, ref 23; $\triangledown$, ref 21 using the rate constant for the recombination of C_6H_5 reported by Park and Lin (ref 17).

agree reasonably well with the expression recommended by Tsang and Kiefer, $k_5 = 2.5 \times 10^{13}(300/T)^{0.3}$ cm^3/(mol·s).[30] A more detailed discussion on k_5 determined by this and other related experiments will be presented elsewhere.[29]

IV. Concluding Remarks

In this investigation, two complementary experimental techniques (pyrolysis/FTIR and PLP/MS) have been developed for the kinetic study of C_6H_5 radical reactions. These techniques have effectively extended the range of temperature from the upper limit of the cavity ringdown method (523 K) to 1000 K. The values of a rate constant covering the wide temperature range of $300-1000$ K can be utilized for a reliable extrapolation to the combustion regime ($1500-2500$ K), particularly with the aid of the TST or the RRKM theory using transition-state parameters obtained by high-level ab initio MO calculations as has been demonstrated in the present $C_6H_5 + H_2$ case.

For the $C_6H_5 + H_2$ reaction, the results determined with the two techniques covering the temperature range $548-1017$ K agree closely with the theoretically predicted rate constant, $k = 5.72 \times 10^4 T^{2.43} \exp(-3159/T)$ cm^3/(mol·s), by Mebel et al.[19] and with the results of a shock tube study by Troe and co-workers[20] in the temperature range of $1050-1450$ K using UV absorption spectroscopy. The above expression is recommended for combustion modeling.

References and Notes

(1) Glassman, I. *Combustion*, 2nd ed.; Academic Press: New York, 1986.

(2) Bittner, J. D.; Howard, J. B. *18th Symposium (International) on Combustion, [Proceedings]*; The Combustion Institute: Pittsburgh, 1983; p 1105.

(3) Brezinsky, K.; Litzinger, T. A.; Glassman, I. *Int. J. Chem. Kinet.* **1984**, *16*, 1053.

(4) Sawyer, R. F. *24th Symposium (International) on Combustion, [Proceedings]*; The Combustion Institute: Pittsburgh, 1992; p 1423.

(5) Bockhorn, H. *Soot Formation in Combustion*; Springer-Verlag: New York 1993.

(6) Yu, T.; Lin, M. C. *J. Am. Chem. Soc.* **1993**, *115*, 4371.

(7) Lin, M. C.; Yu, T. *Int. J. Chem. Kinet.* **1993**, *25,* 875.

Rate Constant for the C$_6$H$_5$ + H$_2$ Reaction

J. Phys. Chem. A, Vol. 101, No. 47, 1997 **8843**

(8) Yu, T.; Lin, M. C. *J. Phys. Chem.* **1994**, *98*, 2105.

(9) Yu, T.; Lin, M. C. *Int. J. Chem. Kinet.* **1994**, *26*, 771.

(10) Yu, T.; Lin, M. C. *J. Phys. Chem.* **1994**, *98*, 9697.

(11) Yu, T.; Lin, M. C. *Int. J. Chem. Kinet.* **1994**, *26*, 1095.

(12) Yu, T.; Lin, M. C. *J. Am. Chem. Soc.* **1994**, *116*, 9571.

(13) Yu, T.; Mebel, A. M.; Lin, M. C. *J. Phys. Org. Chem.* **1995**, *8*, 47.

(14) Yu, T.; Lin, M. C. *Combust. Flame* **1995**, *100*, 169.

(15) Yu, T.; Lin, M. C. *J. Phys. Chem.* **1995**, *99*, 8599.

(16) Park, J.; Lin, M. C. *J. Phys. Chem. A* **1997**, *101*, 14.

(17) Park, J.; Lin, M. C. *J. Phys. Chem. A* **1997**, *101*, 19.

(18) Park, J.; Lin, M. C. *J. Phys. Chem. A* **1997**, *101*, 2643.

(19) Mebel, A. M.; Lin, M. C.; Yu, T; Morokuma, K. *J. Phys. Chem. A* **1997**, 101, 3189.

(20) Heckmann, E.; Hippler, H.; Troe, J. *26th Symposium (International) on Combustion, [Proceedings]*; The Combustion Institute: Pittsburgh, PA, 1996; p 543.

(21) Fielding, W.; Pritchard, H. O. *J. Phys. Chem.* **1962**, *66*, 821.

(22) Asaba, T.; Fujii, T. *Proc. Int. Shock Tube Symp.* **1971**, *8*, 1.

(23) Kiefer, J. H.; Mizerka, L. J.; Patel, M. R.; Wei, H. C. *J. Phys. Chem.* **1985**, *89*, 2013.

(24) Rao, V. S.; Skinner, G. B. *J. Phys. Chem.* **1984**, *88*, 5990.

(25) Halbgewachs, M. J.; Diau, E. W. G.; Mebel, A. M.; Lin, M. C.; Melius, C. F. *26th Symposium (International) on Combustion, [Proceedings]*; The Combustion Institute: Pittsburgh, PA, 1996; p 2109.

(26) Park, J.; Dyakov, I. V.; Mebel, A. M.; Lin, M. C. *J. Phys. Chem. A* **1997**, *101*, 6043.

(27) Wyatt, J. R.; DeCorpo, J. J.; McDowell, M. V.; Saalfeld, F. E. *Rev. Sci. Instrum.* **1974**, *45*, 916.

(28) Wyatt, J. R.; DeCorpo, J. J.; McDowell, M. V.; Saalfeld, F. E. *Int. J. Mass Spectrom. Ion Phys.* **1975**, *16*, 33.

(29) Park, J.; Dyakov, I. V.; Lin, M. C. To be published.

(30) Tsang, W.; Kiefer, J. H. In *Chemical Dynamics and Kinetics of Small Radicals*; Liu, K., Wagner, A. F., Eds.; World Scientific: Singapore, 1996; Part I, p 58.

(31) Baulch, D. L.; Cobos, C. J.; Cox, R. A.; Esser, C.; Frank, P.; Just, Th.; Kerr, J. A.; Pilling, M. J.; Troe, J.; Walker, R. W.; Warnatz, J. *J. Phys. Chem. Ref. Data* **1992**, *21*, 734.

(32) Tsang, W.; Hampton, R. F. *J. Phys. Chem. Ref. Data* **1986**, *15*, 1087.

(33) Duncan, F. J.; Trotman-Dickenson, A. F. *J. Chem. Soc.* **1962**, 4672.